

# Interlayer stacking and nature of the electronic band gap in graphitic BC<sub>2</sub>N: First-principles pseudopotential calculations

Zicheng Pan,<sup>1</sup> Hong Sun,<sup>1,2,\*†</sup> and Changfeng Chen<sup>2,\*‡</sup>

<sup>1</sup>Department of Physics, Shanghai Jiao Tong University, Shanghai 200030, China

<sup>2</sup>Department of Physics and High Pressure Science and Engineering Center, University of Nevada, Las Vegas, Nevada 89154, USA

(Received 26 January 2006; published 9 May 2006)

Using first-principles calculations we establish the equilibrium structure and resolve the dispute on the nature of the electronic band gap of the layer-structured graphitic BC<sub>2</sub>N. The calculated results clearly indicate the indirect nature of the band gap and provide a quantitative account for the band gap and the dispersion of the conduction band near the valence band top observed in recent experiments. These results demonstrate the crucial role of the interlayer interaction and the stacking in determining the electronic property of graphitic BC<sub>2</sub>N.

DOI: [10.1103/PhysRevB.73.193304](https://doi.org/10.1103/PhysRevB.73.193304)

PACS number(s): 71.20.-b, 63.20.Dj, 81.05.Zx

The ternary BCN materials have attracted considerable interest in recent years.<sup>1–6</sup> Among them the layer-structured graphitic BC<sub>2</sub>N (g-BC<sub>2</sub>N) has received special attention since it is a *p*-type semiconductor with a particularly reliable composition in the chemical vapor deposited thin film fabrication. Fundamental issues regarding its structural and electronic properties have been explored but remain unresolved. An earlier experiment<sup>4</sup> concluded that g-BC<sub>2</sub>N has a direct band gap. However, it is contradicted by a later experiment under identical synthesis conditions<sup>6</sup> that indicated that g-BC<sub>2</sub>N is an indirect band-gap semiconductor. On the theoretical side, the situation is also unclear. An earlier first-principles calculation<sup>7</sup> was performed for a single graphitic BC<sub>2</sub>N sheet (i.e., a *monolayer* structure). The calculated electronic band structure is somewhat ambiguous on the nature of the band gap since the lowest conduction band edge cannot be clearly identified. Common wisdom seems to suggest that the interlayer interaction is weak and unlikely to have an impact on the qualitative physics in g-BC<sub>2</sub>N; as a result, the theoretical work on the monolayer<sup>7</sup> has been cited to discuss *both* direct<sup>4</sup> and indirect<sup>6</sup> band gap scenarios in bulk g-BC<sub>2</sub>N. However, the interlayer stacking and its role in determining the electronic properties remain unexplored.

In this paper we report on an *ab initio* study of the structural and electronic properties of the graphitic BC<sub>2</sub>N. We conducted an extensive examination of possible stacking options and identified, based on first-principles total-energy and dynamic phonon calculations, several stable structures close in energy but with different stacking positions. The stacking variations lead to significant differences in electronic band structures, particularly in the dispersion of the conduction band near the valence band top. Furthermore, we show that, contrary to previous results, the monolayer g-BC<sub>2</sub>N is clearly a direct band-gap semiconductor and the interlayer interaction introduces substantial modifications in the dispersion that alter the nature of the band gap.

The total-energy calculations have been carried out using the local-density-approximation (LDA) pseudopotential scheme with a plane-wave basis set<sup>8–10</sup> and a cut-off energy of 80 Ry. The norm-conserving Troullier-Martins pseudopotentials<sup>11</sup> were used with a cut-off radii of 1.3, 1.3,

1.5 a.u. for N, C, and B, respectively. The total energy of the structures is minimized by relaxing the structural parameters using a quasi-Newton method.<sup>12</sup> Phonon modes of the crystal structure were calculated with the linear response theory<sup>13</sup> using the ABINIT code for the equilibrium structures obtained after the structural relaxation. This approach has been applied to systems containing B, C, and N, including layered graphitic structures, with good accuracies on structural parameters and phonon frequencies.<sup>14,15</sup> Although LDA cannot describe the van der Waals interactions between the layers, the accurate predictions of the graphitic phases of carbon,<sup>16,17</sup> boron nitride,<sup>18</sup> and BC<sub>3</sub>,<sup>15</sup> particularly the interlayer distance and the phonon frequency corresponding to the parallel relative motion of the layers, indicate that the short-ranged interactions in these structures are described adequately by LDA. We expect this also to be the case for the layered graphitic BC<sub>2</sub>N structures given their close similarity in structural and bonding characters.

The unit cell on one g-BC<sub>2</sub>N layer in Fig. 1(a) is the lowest-energy monolayer structure, in agreement with an earlier calculation.<sup>7</sup> To examine the interlayer stacking in ABAB... sequences, we have chosen, within the symmetry constraint of the system, a set of twelve initial positions for the center of the unit cell (CUC) of one layer relative to the

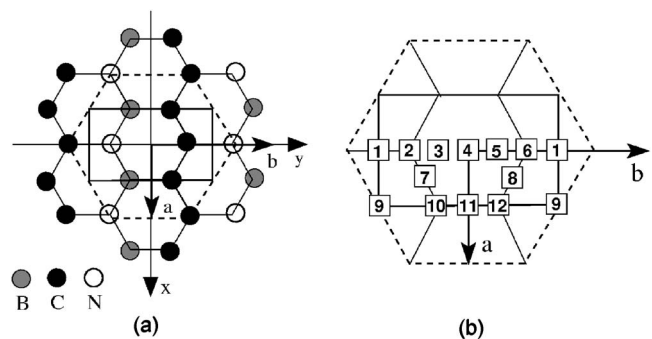


FIG. 1. (a) The unit cell on one layer of g-BC<sub>2</sub>N. (b) The initial interlayer stacking positions. The numbered squares indicate the locations of the center of the unit cell of one layer relative to the adjacent layer before the structural relaxation.

TABLE I. Structural relaxation pattern and number of imaginary phonon modes (at  $\Gamma$ ) for the 20 g-BC<sub>2</sub>N configurations.

Initial position	Final position	Relaxation convergence	Imaginary phonon modes
A1	A1	Yes	1
A2, A3	A2	Yes	0
A4	A4	Yes	2
A7		No	
A9	A9	Yes	2
A11	A11	Yes	1
A12	A12	Yes	0
B1, B2, B3, B7	B2	Yes	0
B4, B5, B6	B5	Yes	1
B8, B11, B12	B12	Yes	0
B9		No	
B10	B10	Yes	2

adjacent layer as shown in Fig. 1(b). There are two topologically distinct options to orient adjacent layers. Stacking option A simply introduces the shifts of CUC of layer *B* relative to that of layer *A* as indicated in Fig. 1(b); option B first exchanges the positions of N and B atoms in layer *B* before making the same initial shifts of CUC relative to layer *A*. The difference between these two options can also be viewed from the local bonding environment, namely, the orientations of the C-N (or C-B) bonds in adjacent layers, which are parallel (option A) or antiparallel (option B) to each other, respectively. In option A, there is a C<sub>2</sub> operation with respect to the *y* axis which renders positions 5, 6, 8, and 12 equivalent to positions 3, 2, 7, 10, respectively. This symmetry is lost in option B due to the difference in local bonding environments. Consequently, we consider a total number of 20 initial stacking configurations.

We carried out first-principles total-energy calculations with full structural relaxations for all 20 configurations and performed dynamic phonon calculations (at  $\Gamma$ ) on all the converged structures to test their dynamic stability. The results are summarized in Table I. This extensive search yields four stable configurations; their total energies and fully relaxed structural parameters are given in Table II. Among them stacking position A2 is the most common type for a

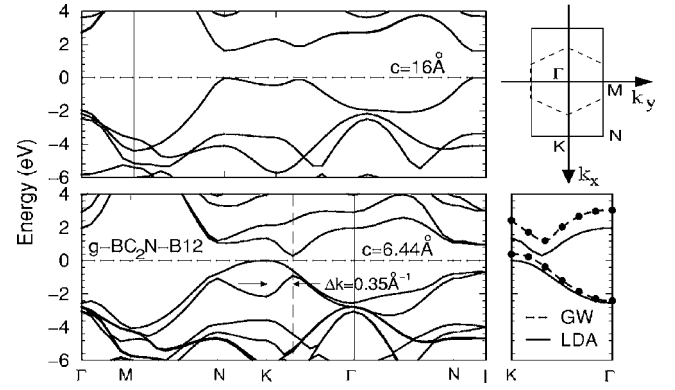


FIG. 2. The calculated electronic band structure of g-BC<sub>2</sub>N-B12 in the equilibrium structure ( $c=6.44$  Å) and an artificially expanded (along the *c*-axis) structure. The *k*-vectors are defined in the upper right panel; point I is above point N along the *k<sub>z</sub>* axis. The vertical dashed line indicates the position of the conduction band bottom. The different scales of the reciprocal space are due to the change in the interlayer distance. The GW results along *K*- $\Gamma$  for the bottom conduction band and top valence band compared to the LDA results are shown in the lower right panel.

graphitic structure while position B12 is unusual in that adjacent layers are different in topology with opposite orientations for the C-N (or C-B) bonds. Our calculated lattice parameters compare well (within 1% for *a* and 3%–5% for *c*) with available experimental data<sup>19,20</sup> and slightly underestimate them as is typical for LDA calculations. It should be noted that the experimental data are extracted assuming an ideal hcp structure (i.e.,  $b/a=1.732$ ) while our fully relaxed structural data deviate slightly from this ideal arrangement. Despite that the four structures are close in energy, we will show below that only the lowest-energy structure, g-BC<sub>2</sub>N-B12, with the unusual stacking provides a quantitative account for the key features of the electronic properties observed in the reported experiments.<sup>4,6</sup>

Figure 2 shows the calculated electronic band structure of g-BC<sub>2</sub>N-B12 in the equilibrium structure along with that in an expanded (along the *c*-axis) structure. At  $c=16.0$  Å, the latter is essentially equivalent to a monolayer with little interlayer interactions as clearly indicated by the dispersionless bands along the N-I direction. In this case, g-BC<sub>2</sub>N is clearly a direct band-gap (of 1.5 eV) semiconductor. As *c* is reduced to its equilibrium value, significant changes occur in the band structure. A strong dispersion develops along the N-I

TABLE II. Calculated total energies and structural parameters. *a* and *b* are indicated in Fig. 1(a), and  $c/2$  is the interlayer distance.  $x_0$  and  $y_0$  are the coordinates of the center of the unit cell of one layer relative to that of the adjacent layer in the fully relaxed structure.

	<i>E</i> (eV/atom)	<i>a</i> (Å)	<i>b</i> (Å)	<i>c</i> /2 (Å)	$x_0$ (Å)	$y_0$ (Å)
g-BC <sub>2</sub> N-A2	-165.3179	2.466	4.323	3.239	0	-1.692
g-BC <sub>2</sub> N-A12	-165.3130	2.465	4.324	3.307	1.233	0.908
g-BC <sub>2</sub> N-B2	-165.3151	2.465	4.324	3.249	0	-1.479
g-BC <sub>2</sub> N-B12	-165.3191	2.465	4.323	3.218	1.233	0.818
Experiment		2.475		3.38		
(Refs. 19 and 20)		2.482		3.310		

direction, indicating substantial interlayer interactions. The valence band top at the N point drops by about 1.0 eV which shifts the top of the valence band toward the K point. Meanwhile, even more pronounced changes occur in the conduction band. While the original conduction band bottom at the N point also drops by about 1.0 eV, maintaining a 1.5 eV gap at the N point, the conduction band bottom near the K point (along  $K-\Gamma$ ) drops by about 1.5 eV with a steep dispersion. The resulting band structure has an indirect gap, in agreement with recent experiment.<sup>6</sup> Moreover, the calculated downward dispersion of 1.0 eV of the conduction band from the K point to its bottom over a change of  $\Delta k=0.35 \text{ \AA}^{-1}$  is in good agreement with the experimentally determined<sup>6</sup> dispersion of 0.7 eV over  $\Delta k=0.32 \text{ \AA}^{-1}$ . For further comparison, we performed GW calculations<sup>21</sup> for the bottom conduction band and top valence band along  $K-\Gamma$ . The GW vertical band gap increases from the LDA value of 1.4 eV to 2.05 eV which is in excellent agreement with the experimental value of 2.1 eV.<sup>4</sup> The GW indirect band gap of 0.82 eV is somewhat smaller than the experimental value of  $1.4\pm 0.1$  eV.<sup>6</sup> A possible source for this discrepancy is that the samples used in the experiment may not have exactly the same stoichiometry and atomic structure as those considered in the present paper. Most importantly, it is noted that the GW calculation has little effect on the LDA band dispersion. Consequently, the LDA dispersion can serve to discriminate among different  $g\text{-BC}_2\text{N}$  structures with distinct interlayer stacking configurations.

Figure 3 shows the band structures of the other three stable configurations of  $g\text{-BC}_2\text{N}$ . None of them fits the experimental results.<sup>6</sup> In the case of  $g\text{-BC}_2\text{N-A2}$ , the downward shift of the valence band top and the conduction band bottom at the N point and the development of the new valence band top at the K point are similar to those in Fig. 2, but the conduction band near the K point (along  $K-\Gamma$ ) drops by only 0.5 eV, leaving the bottom of the conduction band still at the N point as shown in the top panel of Fig. 3. More significantly, it results in a very weak dispersion of the conduction band in the vicinity of the valence band top; within the experimental range of  $\Delta k=0.32 \text{ \AA}^{-1}$  the dispersion is only 0.15 eV which is almost a factor of five smaller than the experimental value of 0.7 eV.<sup>6</sup> The band structures of  $g\text{-BC}_2\text{N-A12}$  and  $g\text{-BC}_2\text{N-B12}$  also do not fit the experimentally observed features. It is clearly seen in Fig. 3 that  $g\text{-BC}_2\text{N-A12}$  has a direct band gap near the N point and the conduction band dispersion in the vicinity of the valence

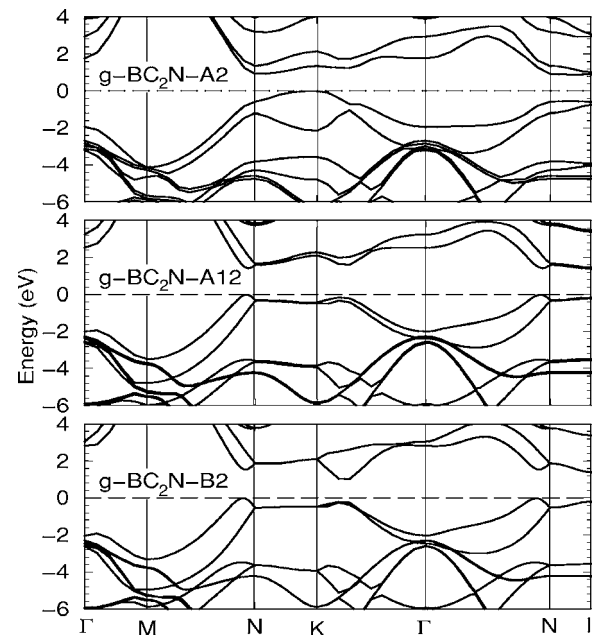


FIG. 3. The calculated electronic band structures of  $g\text{-BC}_2\text{N-A2}$ ,  $g\text{-BC}_2\text{N-A12}$ , and  $g\text{-BC}_2\text{N-B2}$  in their equilibrium structures.

band top is upward, which is opposite to that observed in the experiment. Meanwhile  $g\text{-BC}_2\text{N-B2}$  is an indirect band-gap semiconductor, but its conduction band bottom is too far away from the valence band top to account for the experimentally measured dispersion. Consequently, these three structures are ruled out, leaving only  $g\text{-BC}_2\text{N-B12}$  as the structural assignment for the experimentally synthesized graphitic  $\text{BC}_2\text{N}$ .

In summary, our first-principles total-energy and dynamic phonon calculations have established the equilibrium structure of  $g\text{-BC}_2\text{N}$ . The results resolve the dispute on the nature of the band gap in  $g\text{-BC}_2\text{N}$  and highlight the importance of the interlayer interaction that is usually considered weak but turns out dominating some key features of the electronic band structure.

This work was supported by the Department of Energy under Grants No. DE-FC52-01NV14049 and No. DE-FG36-05GO85028. H.S. was also supported by the National Natural Science Foundation of China under Grants No. 10574089 and No. 50532020 and the High Performance Computing Center at Shanghai Jiao Tong University.

\*Corresponding authors.

†Electronic address: hsun@sju.edu.cn

‡Electronic address: chen@physics.unlv.edu

<sup>1</sup>O. Stephan, P. M. Ajayan, C. Colliex, Ph. Redlien, J. M. Lambert, P. Bernier, and P. Lefin, *Science* **266**, 1683 (1994).

<sup>2</sup>Z. Weng-Sieh, K. Cherrey, N. G. Chopra, X. Blase, Y. Miyamoto, A. Rubio, M. L. Cohen, S. G. Louie, A. Zettl, and R. Gronsky, *Phys. Rev. B* **51**, 11229 (1995).

<sup>3</sup>Ph. Redlich, J. Loeffler, P. M. Ajayan, J. Bill, F. Aldinger, and M. Rühle, *Chem. Phys. Lett.* **260**, 465 (1996).

<sup>4</sup>M. O. Watanabe, S. Itoh, T. Sasaki, and K. Mizushima, *Phys. Rev. Lett.* **77**, 187 (1996).

<sup>5</sup>O. Stephan, Y. Bando, C. Dussarrat, K. Kurashima, T. Sasaki, T. Tamiya, and M. Akaishi, *Appl. Phys. Lett.* **70**, 2383 (1997).

<sup>6</sup>Y. Chen, J. C. Barnard, R. E. Palmer, M. O. Watanabe, and T. Sasaki, *Phys. Rev. Lett.* **83**, 2406 (1999).

- <sup>7</sup>A. Y. Liu, R. M. Wentzcovitch, and M. L. Cohen, Phys. Rev. B **39**, 1760 (1989).
- <sup>8</sup>J. Ihm, A. Zunger, and M. L. Cohen, J. Phys. C **12**, 4409 (1979).
- <sup>9</sup>D. M. Ceperley and B. J. Alder, Phys. Rev. Lett. **45**, 566 (1980).
- <sup>10</sup>M. L. Cohen, Phys. Scr., T **1**, 5 (1982).
- <sup>11</sup>N. Troullier and J. L. Martins, Phys. Rev. B **43**, 1993 (1991).
- <sup>12</sup>B. G. Pfrommer, M. Cote, S. G. Louie, and M. L. Cohen, J. Comput. Phys. **131**, 233 (1997).
- <sup>13</sup>X. Gonze, Phys. Rev. B **55**, 10337 (1997); X. Gonze and C. Lee, *ibid.* **55**, 10355 (1997).
- <sup>14</sup>H. Sun, S. H. Jhi, D. Roundy, M. L. Cohen, and S. G. Louie, Phys. Rev. B **64**, 094108 (2001).
- <sup>15</sup>H. Sun, F. J. Ribeiro, J. L. Li, D. Roundy, M. L. Cohen, and S. G. Louie, Phys. Rev. B **69**, 024110 (2004).
- <sup>16</sup>M. C. Schabel and J. L. Martins, Phys. Rev. B **46**, 7185 (1992).
- <sup>17</sup>J. C. Charlier, X. Gonze, and J. P. Michenaud, Europhys. Lett. **28**, 403 (1994).
- <sup>18</sup>E. Kim and C. F. Chen, Phys. Lett. A **319**, 384 (2003).
- <sup>19</sup>K. Yamada, J. Am. Ceram. Soc. **81**, 1941 (1998).
- <sup>20</sup>J. P. Nicolich, F. Hofer, G. Brey, and R. Riedel, J. Am. Ceram. Soc. **84**, 279 (2001).
- <sup>21</sup>W. G. Aulbur, L. Jonsson, and J. W. Wilkins, Solid State Phys. **54**, 1 (2000).